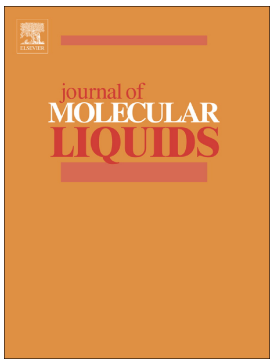


# MWCNTs-Fe3O4 nanocomposite for Hg(II) high adsorption efficiency

Hamidreza Sadegh, Gomaa A.M. Ali, Abdel Salam Hamdy Makhlouf, Kwok Feng Chong, Njud S. Alharbi, Shilpi Agarwal, Vinod Kumar Gupta

PII: S0167-7322(18)30223-X
DOI: doi:10.1016/j.molliq.2018.03.012
Reference: MOLLIQ 8786

To appear in: *Journal of Molecular Liquids*

Received date: 14 January 2018
Revised date: 21 February 2018
Accepted date: 3 March 2018

Please cite this article as: Hamidreza Sadegh, Gomaa A.M. Ali, Abdel Salam Hamdy Makhlouf, Kwok Feng Chong, Njud S. Alharbi, Shilpi Agarwal, Vinod Kumar Gupta , MWCNTs-Fe3O4 nanocomposite for Hg(II) high adsorption efficiency. The address for the corresponding author was captured as affiliation for all authors. Please check if appropriate. Molliq(2017), doi:10.1016/j.molliq.2018.03.012

# MWCNTs-$Fe_3O_4$ Nanocomposite for Hg(II) High Adsorption Efficiency

**Hamidreza Sadegh [a,*], Gomaa A. M. Ali [b,c,d,*], Abdel Salam Hamdy Makhlouf [e], Kwok Feng Chong [d], Njud S. Alharbi [g], Shilpi Agarwal [e], Vinod Kumar Gupta [f,g,*]**

[a] West Pomeranian University of Technology, Szczecin, Faculty of Chemical Technology and Engineering, Division of Biomaterials and Microbiological Technologies, Al. Piastow 45, Szczecin, Poland

[b] Chemistry Department, Faculty of Science, Al-Azhar University, Assiut, 71524, Egypt

[c] Al-Azhar Center of Nanoscience and Applications (ACNA), Al-Azhar University, Assiut, 71524, Egypt

[d] Faculty of Industrial Sciences & Technology, Universiti Malaysia Pahang, Gambang, 26300 Kuantan, Malaysia

[e] Department of Manufacturing and Industrial Engineering, College of Engineering and Computer Science, University of Texas Rio Grande Valley, 1201 West University Dr., Edinburg, TX 78541-2999, USA

[f] Department of Applied Chemistry, University of Johannesburg, Johannesburg, South Africa

[g] Department of Biological Sciences, King Abdulaziz University, Jeddah 21589, Saudi Arabia

[*]Corresponding authors:

*hamid-sadegh@zut.edu.pl* (H.Sadegh),

*gomaasanad@azhar.edu.eg*, *gomaasaand@gmail.com* (G.A.M. Ali)

*vinodfcy@gmail.com* (V. K Gupta)

**Abstract**

Magnetic carbon nanotubes composite (MWCNTs-$Fe_3O_4$) was successfully prepared and characterized using different techniques. MWCNTs-$Fe_3O_4$ displays entangled network of oxidized MWCNTs attached with $Fe_3O_4$ clusters with specific surface area of 92 $m^2$ $g^{-1}$. The adsorption performance of as prepared composite was investigated for Hg(II) removal. Several experimental factors affecting Hg(II) adsorption process by MWCNTs-$Fe_3O_4$ were studied including, adsorbent dosage, contact time, pH and metal ion concentration. A high adsorption capacity of 238.78 mg $g^{-1}$ was obtained according to Langmuir model. In addition, pseudo-second-order and the Langmuir isotherm model were used to fit the adsorption kinetic and equilibrium data, respectively. The results recommend the successful application of MWCNTs-$Fe_3O_4$ for Hg(II) removal via batch adsorption technique.

***Keywords:*** Carbon nanotubes, Nanocomposite, Water treatment, Adsorption, Hg(II) removal, Pollutants.

## 1. Introduction

A serious environmental problem of increasing interest is the heavy metals contamination of aqueous media and industrial effluents because of the toxic nature and accumulation of these metal ions in the food chain, and the subsequent non-biodegradability [1]. Rapid industrialization is the main source for releasing toxic heavy metals to the environment. The major sources of heavy metal ion contaminations are mining industry, battery manufacturing, electroplating, textile industry, petroleum refining, paint manufacture, photographic industries, etc [1, 2]. Due to its

toxicity, long-range transport, persistence and bioaccumulation in the environment, mercury (Hg) is considered as one of the most important environmental contaminants that have caused global concerns [3]. Thus, the removal of such toxic materials from wastewater is becoming a crucial issue. Many physical, biological and chemical techniques have been developed to control this issue [4-8]. Due to its high efficiency and economic consideration, adsorption process was proved to be the most efficient technique [9-11]. In addition, adsorption technique has no harmful effect and doesn't produce harmful substances [12-15]. Adsorbents materials such as zeolites, polymers, biomaterials, have been tested and examined for possible application of toxic heavy metal ions adsorption [16-19]. Nowadays, developing of effective adsorbents is of increasing global interest for the water treatment application since the adsorption efficiency is mostly depending on the adsorbent properties [16, 17, 20-22]. Therefore, development of more efficient adsorbents has gained the attention of quite a large number of researchers. New nanomaterials-based adsorbents have been proposed as novel adsorbents for the removal of heavy metal ions from wastewater with better adsorption performance [10, 23-25].

Carbon nanotubes (CNTs) have pulled in significant interdisciplinary interest on account of their one of exclusive chemical and physical properties; however, the known hydrophobicity of CNTs could restrict some of their applications [26, 27]. Accordingly, treatments of CNTs with specific functional groups or nanoparticles could have the potential to overcome these drawbacks and widen the applications of CNTs [28-30]. Magnetic metal oxide nanoparticles have been reported as efficient, highly effective and economic adsorbents. Moreover, they are easy to separate under a magnetic field for recovering [31-34]. Metal oxide/non-metal nanocomposites show good enhancement of adsorption efficiency of methylene blue because of their high surface

area and lower particles size [10]. Therefore, nanocomposites of metal oxide and CNTs would be very effective in adsorption process as it possesses unique morphological properties.

This paper discusses the preparation and characterization of a novel nanocomposite adsorbent for the adsorption of Hg(II). The idea is to overcome the known hydrophobicity of multi-walled carbon nanotubes (MWCNTs) through surface treatment of MWCNTs with magnetic $Fe_3O_4$ nanoparticles. Several experimental parameters such as adsorbent dosage, pH, contact time, metal ion concentration etc, and their effect on the adsorption efficiency will be studied. The objectives of this paper are: (i) to study the efficiency of MWCNTs-$Fe_3O_4$ as an adsorbent for the adsorption of Hg(II), (ii) to find out the best-fit isotherm model (Langmuir and Freundlich), and (iii) to determine the kinetic parameters that affecting and controlling the adsorption process.

## 2. Experimental

### *2.1 Materials*

MWCNTs were obtained from NanoAmor Nanostructured & Amorphous Materials, Inc, USA. Chemical vapor deposition (CVD) method was used to prepare MWCNTs with the specification of purity of 95%, outer diameters of 50 nm, length in the range from 500 to 2000 nm and specific surface area of 40 $m^2$ $g^{-1}$. In addition, $HgCl_2$ aqueous solutions with different concentrations were prepared and used as sources for Hg(II). All other reagents and chemicals were provided by Merck Inc, USA.

*2.2 Samples Preparation*

MWCNTs-$Fe_3O_4$ nanocomposite was prepared as reported in our previous work [35]. Briefly, the bare MWCNTs was treated with $HNO_3$ and then exposed to microwave radiation to be functionalized with carboxylic groups as a result of oxidation reaction occurred. $Fe_3O_4$ nanoparticles were prepared by chemical co-precipitation method [36, 37]. The obtained magnetic nanoparticles were mixed with the treated MWCNTs in 40 mL solution of deionized water/ethanol (1:1). The mixture was ultrasonicated for 1 h and stirred for 96 h. A filter membrane of 200 nm was used to separate the solution from the residue, followed by vacuum drying at 50 °C for 16 h. MWCNTs-$Fe_3O_4$ preparation stages are shown in Scheme 1.

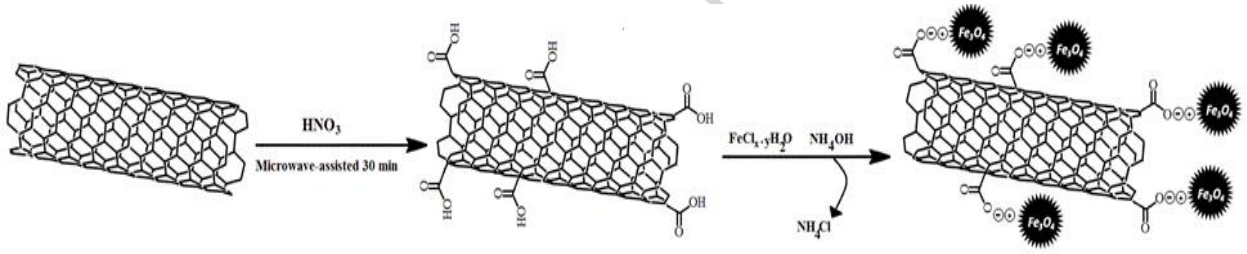


**Scheme 1.** A schematic diagram for the synthesis of MWCNTs-$Fe_3O_4$.

*2.3 Materials Characterization*

The synthesized MWCNTs-$Fe_3O_4$ nanocomposite was examined by Fourier-transform infrared spectroscopy (FTIR), X-ray powder diffraction (XRD) analysis, transmittance electron microscopy (TEM), scanning electron microscopy (SEM), Thermogravimetric analysis (TGA) and vibrating sample magnetometer (VSM). The instrumentation detailed were given elsewhere [35]. The surface area of the synthesized MWCNTs-$Fe_3O_4$ nanocomposite materials was measured using $N_2$ adsorption-desorption techniques.

*2.4 Adsorption Experiments*

A stock solution of Hg(II) (1000 mg $L^{-1}$) was prepared by dissolving $HgCl_2$ in deionized water. To determine the optimum Hg(II) adsorption parameters, the adsorption experiments were conducted in 100 mL stopper conical flask and shaken using a temperature controlled shaker. The effect of different dosages (2-16 mg) was evaluated at 20 mg $L^{-1}$ initial concentration ($C_o$), 2 h contact time, natural pH, and at 25 ºC. The effect of contact time (1-120 min) was also studied at 20 mg $L^{-1}$, 10 mg, natural pH, 25 ºC. The effect of pH from 1-8 was investigated at 20 mg $L^{-1}$, 10 mg, 1 h, 25 ºC. Adsorption equilibrium studies in the single system were performed at 10 - 50 mg $L^{-1}$ initial concentrations. The adsorbent was separated from the solution at the end of the adsorption process using a magnetic separator. The optimum Hg(II) concentration was determined by atomic adsorption spectrophotometer (GBC-932, AAS, Australia). The adsorption capacity ($Q_e$, mg $g^{-1}$) was calculated according to Eq. 1 [11, 15]:

$$Q_e = \frac{(C_o - C_e)V}{m} \quad (1)$$

where $C_o$ & $C_e$ are the initial and equilibrium Hg(II) concentrations (mg $L^{-1}$) respectively. $V$ is the volume of adsorption solution (L), and $m$ is the mass of adsorbent (g).

## 3. Results and Discussion

### 3.1 Characterization of Adsorbent

*3.1.1 Structural Characteristics*

FTIR spectra showed the band at 1580 $cm^{-1}$ indicating the presence of cylinder-like carbon structure. The stretching mode of C=O vibration of the carboxyl group (COOH) is clear from the modified MWCNTs spectrum. The same finding was also observed at 1713 $cm^{-1}$ for MWCNTs-COOH, and at 1724 $cm^{-1}$ for MWCNTs-$Fe_3O_4$. This band has been reduced significantly in case of MWCNTs-$Fe_3O_4$ compared to MWCNTs-COOH. This reduction can be attributed to the formation of a linkage between $Fe_3O_4$ particles and MWCNTs, through a reaction between COOH groups and the magnetite particles. The broad band near 585 $cm^{-1}$ confirms the presence of iron oxide (primary magnetite) in MWCNTs-$Fe_3O_4$ [35, 38]. The phase and crystalline structure of cubic $Fe_3O_4$ and MWCNTs were confirmed by XRD measurement as shown by their characteristics peaks. The main $Fe_3O_4$ peaks are broad, indicating the small crystallite size of $Fe_3O_4$ nanoparticles [39]. According to the Scherrer formula [40], the mean size of $Fe_3O_4$ crystallites was measured to be 10 nm for MWCNTs-$Fe_3O_4$.

*3.1.2 Morphological Characteristics*

SEM, TEM and BET surface area have been used to investigate the morphology of the prepared nanocomposite materials. Fig. 1 shows the SEM images of the prepared materials. According to Fig. 1a and b, MWCNTs-COOH shows an entangled network of oxidized MWCNTs. However, Fig. 1c and d, MWCNTs-$Fe_3O_4$ displays entangled network of oxidized

MWCNTs attached with $Fe_3O_4$ clusters. There is a little increment in the tube diameters due to attached $Fe_3O_4$ nanoparticles on the outer surface.

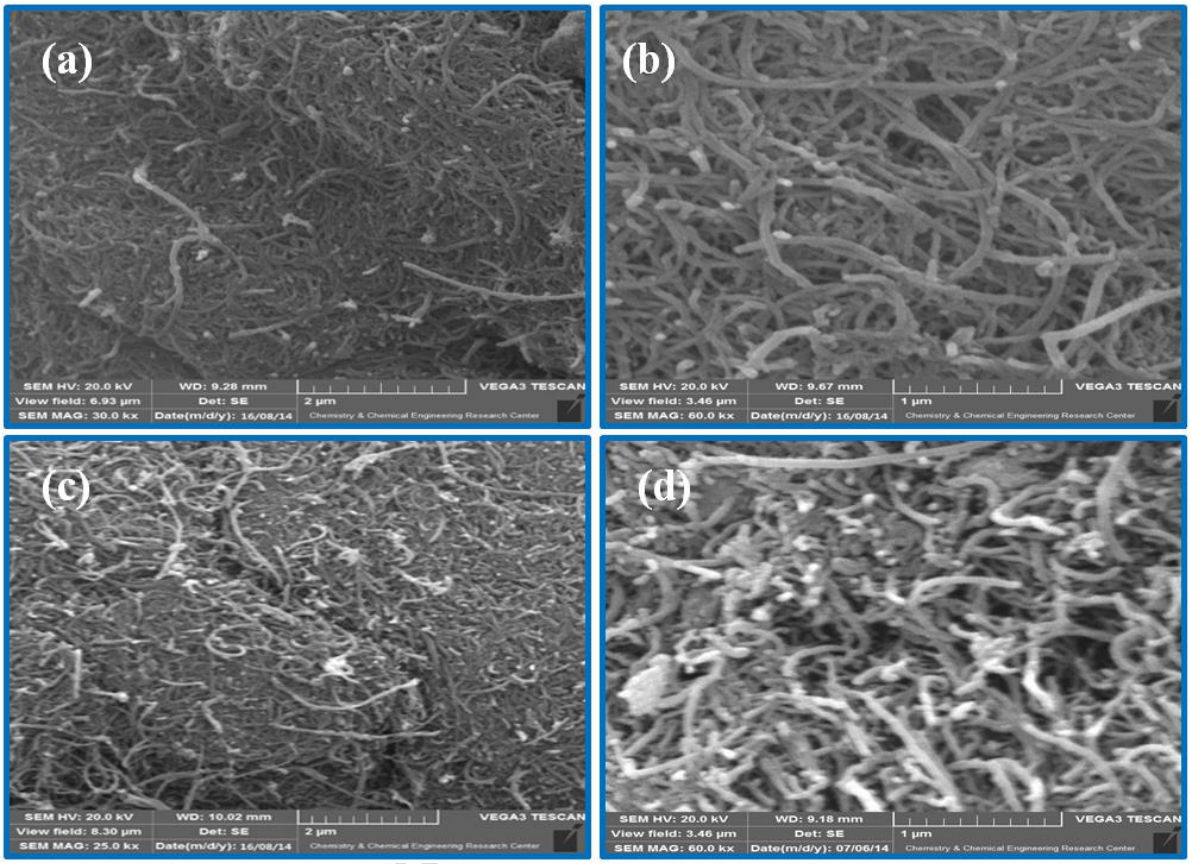


**Fig. 1** SEM micrographs (a), (b) for MWCNTs-COOH, (c) and (d) for MWCNTs-$Fe_3O_4$ at different magnifications.

Further morphological studies were conducted on the prepared materials using TEM (Fig. 2). Fig. 2a shows spherical $Fe_3O_4$ nanoparticles (5-10 nm) which is very close to XRD calculations. In addition, Fig. 2b shows uniform tube structure of MWCNTs. On the other hand, Fig. 2c depicts an entangled network of acidified MWCNTs attached with clusters of $Fe_3O_4$ nanoparticles. The $Fe_3O_4$ nanoparticles aggregates are composed of sub-units of about 10 nm

[41], suggesting that large particles may be formed via precipitation followed by aggregation process. The MWCNTs surface is covered with COOH in which $Fe_3O_4$ nanoparticles are uniformly distributed without aggregation. Carboxylic acid attached to the surface of MWCNTs was stable during the loading iron oxides, because of the simple and easy reaction between carboxylic acid and metal ions due to the presence of a huge number of coordinating functional groups [42]. $Fe_3O_4$ nanoparticles deposit on the defect sites of MWCNTs by spontaneous redox of between $Fe^{3+}$ and the defect sites [43]. The specific surface area of the MWCNTs-$Fe_3O_4$ nanocomposite was found to be 92 $m^2 g^{-1}$. This high surface area is preferable for the adsorption process, where it provides more active centers for the reaction.

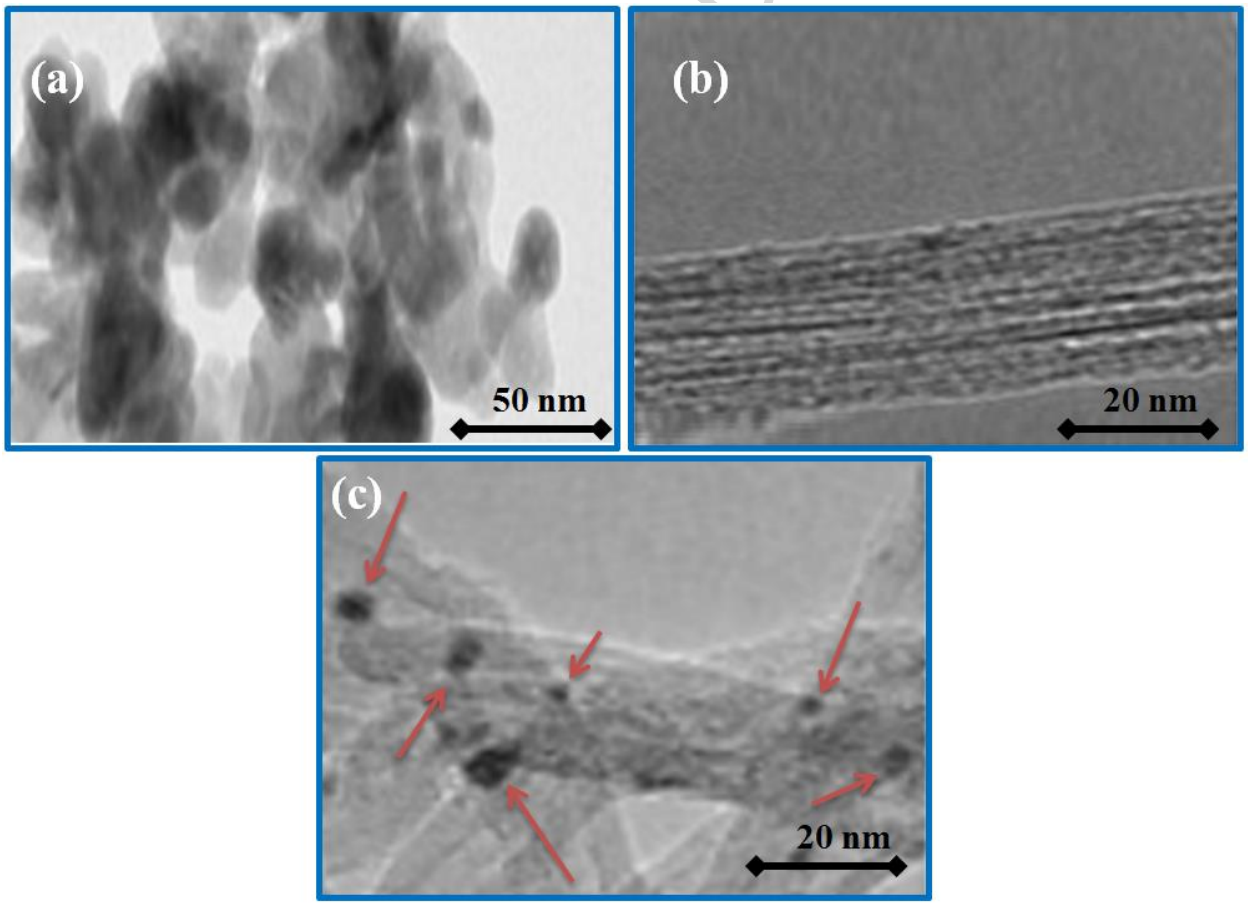

**Fig. 2** TEM images of (a) $Fe_3O_4$, (b) MWCNTs-COOH and (c) MWCNTs-$Fe_3O_4$ nanocomposite.

### 3.2 Adsorption Studies

The presence of a satisfactory amount of adsorbent is essential to determine the number of free adsorption sites at a specific concentration. The experiments were conducted at 25 ºC (MWCNTs-$Fe_3O_4$ dose of 2-16 mg, Hg(II) solution volume and concentration were 25 mL 20 mg $L^{-1}$, respectively). The adsorption of ions increased rapidly with increasing the adsorbent dose (Fig. 3a), due to the enhancement of the active sites with MWCNTs-$Fe_3O_4$. It seems that the adsorption of Hg(II) reached the equilibrium state at 10 mg. Therefore, 10 mg was selected as the optimum adsorbent dosage in this study.

Equilibrium time is an important parameter that should be carefully determined in the design of economical wastewater treatment systems [44]. The effect of contact time on the adsorption process was studied. We conducted the experiments using 10 mg of MWCNTs-$Fe_3O_4$ at natural pH and 25 ºC. From the results shown in Fig. 3b the functionalized magnetic MWCNTs-$Fe_3O_4$ adsorbent exhibit a gradual increase in Hg(II) adsorption capacity with increasing the reaction contact time. The metal adsorption capacity value was found to reach saturation conditions after 60 min by reaching the maximum adsorption of Hg(II). These findings attribute to the binding processes of Hg(II) to the MWCNTs-$Fe_3O_4$ surface via two different steps [45].

The three linear stages as in Fig. 3b illustrate the adsorption process mechanism. The mechanism seems to has three stages: (i) film diffusion stage in which the mass is transferred of

the adsorbent through the water film to the adsorbent surface. (ii) pore diffusion of the adsorbate occurs, and (iii) equilibrium stage in which occupation of a surface site on the adsorbent by physisorption or chemisorption occurs [46]. The adsorption rate of each stage could be correlated to its slope. The first stage can be seen to be the fastest, involving external diffusion to the surface of the adsorbent. It is related to a gradual increase in the metal capacity with the increase of the contact time from 1 to 60 min because of the occupation of the functional groups of the absorbents by the target metal ion. The second stage involving pore diffusion is a relatively slower process of gradual adsorption. Due to the decrease in the number of Hg ions in the solution as well as active sites on the adsorbent surface. It is directly related to the equilibrium and saturation conditions which require more than 60 min. Accordingly, 60 min. contact time was selected as the optimum contact time in this study. The third and final stage which shows the attainment of equilibrium is the slowest.

The solution pH is a crucial parameter that affects directly the degree of ionization, the solubility of metal ion, and the adsorbents properties [47]. Fig. 3c shows the extent of Hg(II) adsorption versus pH. The efficiency of Hg(II) adsorption increases with the solution pH at the low pH. The optimum removal efficiency was accomplished at pH 2, then it decreases with increasing the pH values. The adsorption process is linked with the equilibrium because of the difference in the thermodynamic equilibrium for each adsorbate-adsorbent interaction.

When $Fe_3O_4$ nanoparticles are present on MWCNTs surface, the adsorption efficiency increases as confirmed by previous studies [48]. Several mechanisms have been proposed to explain the role of MWCNTs-$Fe_3O_4$ for the adsorption of Hg(II). These mechanisms include complex formation, electrostatic attraction, physical adsorption, and chemical interaction between

Hg(II) ions with the functional groups of MWCNTs-$Fe_3O_4$. However, complex formation and electrostatic attraction between Hg(II) ions and the functional groups of MWCNTs-$Fe_3O_4$ are the most acceptable mechanisms.

The initial ion concentration is another remarkable parameter that affects the adsorption mechanism. In this paper, we studied the effect of different Hg(II) initial concentration (from 10 to 50 mg $L^{-1}$), on the adsorption capacity using MWCNTs-$Fe_3O_4$. According to Fig. 3d, the adsorption of Hg(II) was gradually increased from 249 to 266 mg $g^{-1}$ at the surface of MWCNTs-$Fe_3O_4$. This confirms that MWCNTs-$Fe_3O_4$ surface has an affinity for Hg(II) ions absorbance due to its small particles sizes and high surface area. The maximum adsorption capacity of Hg(II) was 50 mg $g^{-1}$ using MWCNTs-$Fe_3O_4$ adsorbent.

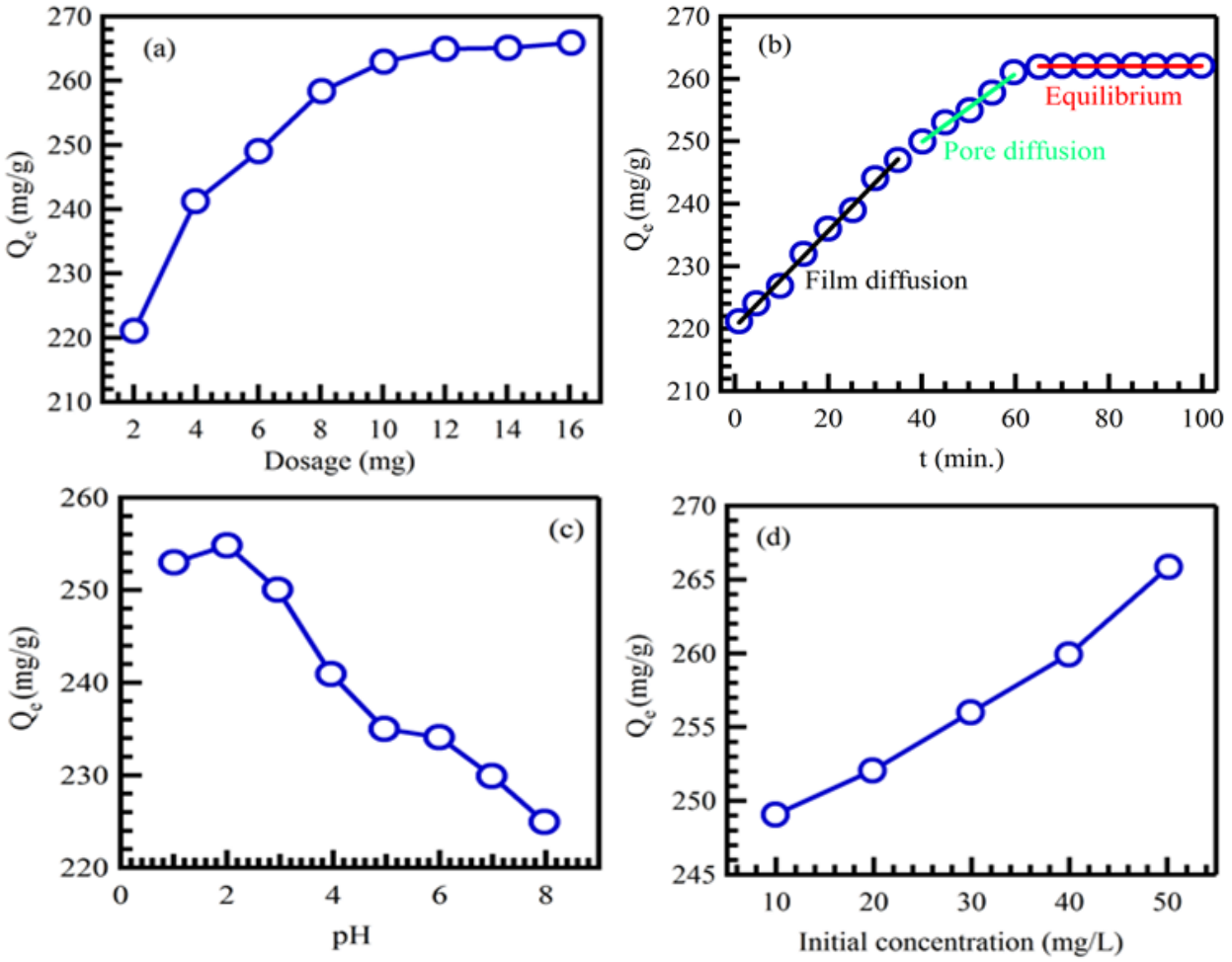


**Fig. 3** Effect of (a) adsorbent dosage (20 mg $L^{-1}$, natural pH, 2 h, 25 ºC), (b) contact time (20 mg $L^{-1}$, 10 mg, natural pH, 25 ºC) (c) pH (20 mg $L^{-1}$, 10 mg, 60 min., 25 ºC) and (d) initial concentration (10 mg, 60 min, pH 2 and 25 ºC). The solid lines are the linear fits.



### 3.3 Adsorption Isotherms

Adsorption isotherms were used to describe the interactive behavior between the adsorbates and adsorbents. To estimate the maximum adsorption capacity ($Q_{max}$ (mg $g^{-1}$)), the equilibrium data were fitted using Langmuir and Freundlich models [49, 50]. The mathematical forms of these models are given by Eqs. 2 and 3, respectively.

$$\frac{C_e}{Q_e} = \frac{1}{Q_{max} K_L} + \frac{C_e}{Q_{max}}$$

(2)

$$\log Q_e = \log K_F + \frac{1}{n} \log C_e$$

(3)

where $Q_e$ is the adsorbate equilibrium amount in solid phases (mg $g^{-1}$), $K_L$ is Langmuir constant (L $mg^{-1}$); $K_F$ (mg $g^{-1}$)(L $mg^{-1})^{1/n}$ and $n$ are Freundlich constants due to adsorption capacity and adsorption intensity, respectively. $Q_{max}$ and $K_L$ can be calculated from the linear plot of $1/Q_e$ versus $1/C_e$ as shown in Fig. 4a. $K_F$ and $1/n$ values can be calculated from the intercept and slope of the linear log $Q_e$ versus log $C_e$ plot as shown in Fig. 4b. The type of isotherm can be determined according to the value of 1/n. Irreversible isotherm can be determined at (1/n = 0). Favorable isotherm can be determined at (0 < 1/n < 1). Unfavorable isotherm can be determined at (1/n > 1) [49].

The linear form of Temkin model was utilized to depict adsorbate-adsorbent connection. The model is represented as Eq. (4) [10, 51]:

$$Q_e = \frac{RT}{2.303 B_T} \log K_T + \frac{RT}{2.303 B_T} \log C_e$$

(4)

where, $R$ is the gas constant (8.314 J $mol^{-1}$ K) and $T$ (K) is the absolute temperature, $B_T$ and $K_T$ are Temkin constants. In addition, Harkin-Jura model represented by Eq. (5) [10, 52] was also applied to fit the experimental data.

$$\frac{1}{Q_e^2} = \frac{B_{HJ}}{A_{HJ}} - \frac{1}{A_{HJ}} \log C_e$$

(5)

where $A_{HJ}$ and $B_{HJ}$ are Harkins-Jura constants. The results of Temkin and Harkin-Jura models are shown in Fig. 4c and d, respectively.

Langmuir isotherm fits better with experimental data which indicates that the adsorbents surfaces are formed from heterogeneous adsorption patches [13] besides less homogeneous patches [53]. Based on the obtained results, the MWCNTs-$Fe_3O_4$ surface has better adsorption efficiency for Hg(II) ions. The favorability of the Hg(II) ions adsorption was evaluated using a dimensionless parameter ($R_L$) as given by Eq. (6):

$$R_L = \frac{1}{1 + K_L Qmax}$$

(6)

Based on the values of $R_L$, the adsorption process can be irreversible ($R_L = 0$), favorable ($0 < R_L < 1$), linear ($R_L = 1$), or unfavorable ($R_L > 1$) [54, 55]. The calculated $R_L$ values for the adsorption of Hg(II) ion using MWCNTs-$Fe_3O_4$ surface is 0.01, therefore, the Hg(II) adsorption onto adsorbent is favorable. The adsorption capacity of MWCNTs-$Fe_3O_4$ was 238.78 mg $g^{-1}$, as calculated by Langmuir equation. Table 1 lists all the isotherm models parameters obtained from the above four models. In addition, Table 2 shows a comparison of the adsorption capacity of the MWCNTs-$Fe_3O_4$ adsorbent with some recent mercury adsorbents based on iron and carbon nanotubes. MWCNTs-$Fe_3O_4$ has better adsorption capacity for Hg(II) than other adsorbents. These high findings are a result of surface functional groups, high surface area, and high porosity corresponded to the superb adsorption capacity and improved adsorption kinetics. This result

suggests the potential of MWCNTs-$Fe_3O_4$ be utilized as a successful adsorbent for the removal of Hg(II) ions in waste/water treatment applications.

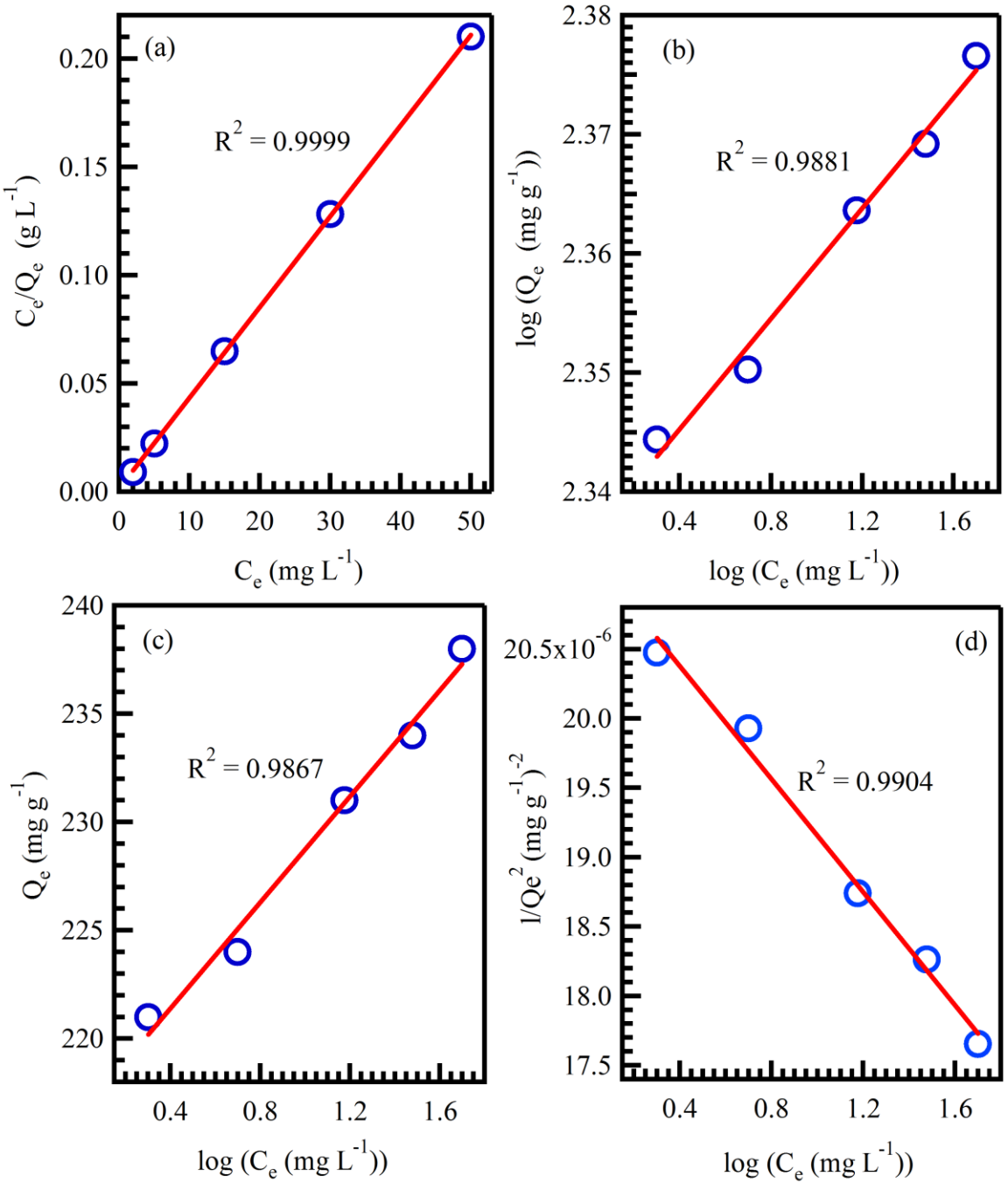


**Fig. 4** Adsorption isotherms for Hg(II) on MWCNTs-$Fe_3O_4$ nanocomposite (a) Freundlich, (b) Langmuir, (c) Temkin and (d) Harkin-Jura. The solid lines are the linear fits.

**Table 1** Fitting parameters of Hg(II) adsorption experimental data to Langmuir, Freundlich, Temkin and Harkin-Jura equations.

| **Model** | **Parameters** | **$R^2$** |
|---|---|---|
| | **$Q_{max}$ = 238.78 mg $g^{-1}$** | |
| **Langmuir** | **$K_L$ = 2.81 L $mg^{-1}$** | **0.9999** |
| | **$R_L$ = 0.002** | |
| | 1/n = 0.43 | |
| Freundlich | $K_F$ = 216.76 mg $g^{-1}$ (L $mg^{-1}$)$^{1/n}$ | 0.9881 |
| Temkin | $B_T$ = 89.46 J $mol^{-1}$ | 0.9867 |
| | $K_T$ = 1.21 L $g^{-1}$ | |
| Harkin-Jura | $A_{HJ}$ = 490.58 $mg^3$ $g^{-2}$ $L^{-1}$ | 0.9904 |
| | $B_{HJ}$ = 0.01 mg $L^{-1}$ | |

**Table 2** Comparison of Hg(II) adsorption capacities using some related nanocomposites adsorbents together with their surface area values.

| **Adsorbent** | **Adsorption capacity ($mg\ g^{-1}$)** | **Surface area ($m^2\ g^{-1}$)** | **Ref.** |
|---|---|---|---|
| $CoFe_2O_4$ coated with polystyrene | 84.30 | 0.71 | [56] |
| $Fe_3O_4$@$SiO_2$-SH nanocomposite | 133.30 | ----- | [57] |
| Polyrhodanine-coated ɣ-$Fe_2O_3$ | 179.00 | 94.65 | [58] |
| Magnetic FeS nanoparticles | 132.00 | 21.30 | [59] |
| Nanoporous carbon impregnated with surfactants | 7.40 | 1179.20 | [60] |
| | 8.10 | 1193.90 | |
| | 8.90 | 1198.40 | |
| SWCNTs-SH | 131.00 | ----- | [61] |
| SWCNTs | 40.16 | ----- | |
| MWCNTs | 0.70 - 3.83 | ----- | [62] |
| MWCNTs | 100.00 | ----- | [63] |
| MWCNTs-Amidoamine | 101.35 | 150.00 | [46] |

| | | | |
|---|---|---|---|
| MWCNTs-with amino and thiol groups | 84.66 | 110.00 | [64] |
| ***MWCNTs-$Fe_3O_4$*** | ***238.78*** | **92.*00*** | ***This work*** |

### 3.4 Adsorption Kinetics

To study the rate of the adsorption process different kinetic models were applied such as pseudo-first-order, pseudo-second-order, intraparticle diffusion and simple Elovich to interpret the experimental data [11, 21, 65, 66]. A linear form of pseudo-first-order model could be given as:

$$\log(Q_e - Q_t) = \log Q_e - \frac{K_1}{2.303} t \quad (7)$$

where, $Q_e$ and $Q_t$ are the amounts of ion adsorbed (mg $g^{-1}$) at equilibrium and time t, respectively. $K_1$ is the equilibrium rate constant ($min^{-1}$). The linear fit between the log ($Q_e$-$Q_t$) and t is shown in Fig. 5a.

Eq. (8) represents the linear form of pseudo-second-order model [67, 68]:

$$\frac{t}{Q_t} = \frac{1}{K_2 Q_e^2} + \frac{1}{Q_e} t \quad (8)$$

where $K_2$ is pseudo-second-order equilibrium constant (g $mg^{-1}$ $min^{-1}$). The linear fit between the $t/Q_t$ and t can be seen in Fig. 5b.

The possible effect due to the intraparticle diffusion resistance on the adsorption was explored using the following model [69]:

$$Q_t = K_D t^{1/2} + D \quad (9)$$

where, $K_D$ is the intraparticle diffusion rate constant and $D$ is the intercept which is related to the

thickness of the boundary layer. According to this model, when intraparticle diffusion is involved in the adsorption process, the plot should be linear and the intraparticle diffusion is the rate determining step if the line pass through the origin [20]. The relation between $Q_t$ and square root of t is shown in Fig. 5c.

The simple Elovich model is expressed by Eq. (10) [10, 70]:

$$Q_t = K_E + \frac{\beta}{2.303}\log t \qquad (10)$$

where $K_E$ represents the rate of chemisorption at zero coverage (mg $g^{-1}$ $min^{-1}$) and $\beta$ is related to the extent of surface coverage and activation energy for chemisorption (g $mg^{-1}$). When $Q_t$ is plotted against log t, a linear relation is obtained as shown in Fig. 5d.

Table 3 shows the kinetic parameters obtained from the experimental data fitting using the above-mentioned equations. According to Table 3, the perfect fitting and the high value of correlation coefficients (>0.999), confirms that the adsorption process follows, with good correlation, the pseudo-second-order model. This suggests that chemisorption is the rate-determining step for Hg(II) ion onto MWCNTs-$Fe_3O_4$, where valency forces are involved because of the electrons sharing or exchange between $Fe_3O_4$ nanoparticles and Hg(II) ions [71].

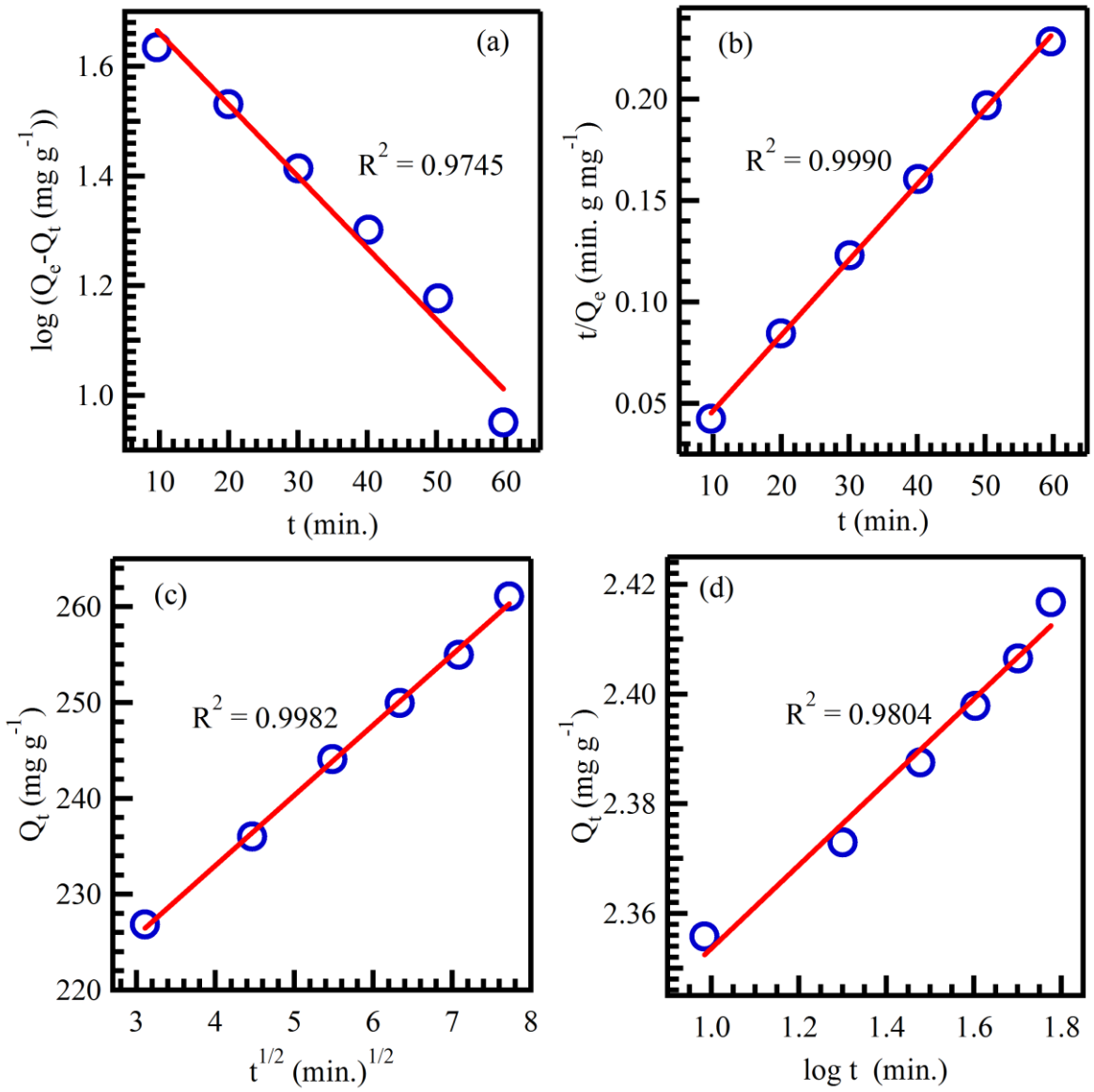


**Fig. 5** Kinetic plots: (a) pseudo-first-order, (b) pseudo-second-order, (c) intraparticle diffusion and (d) simple Elovich models for Hg(II) adsorption on MWCNTs-$Fe_3O_4$ nanocomposite. The solid lines are the linear fits.

**Table 3** The kinetic parameters of Hg(II) adsorption by MWCNTs-$Fe_3O_4$.

| Model | Parameters | $R^2$ |
|---|---|---|
| Pseudo-first-order | $Q_e$ = 61.901 mg $g^{-1}$<br>$K_1$ = 0.030 $min^{-1}$ | 0.9745 |
| **Pseudo-second-order** | **$Q_e$ = 270.270 mg $g^{-1}$**<br>**$K_2$ = 0.002 g $mg^{-1}$ $min^{-1}$** | **0.9990** |
| Intraparticle diffusion | $K_D$ = 7.328 mg $g^{-1}$ $min^{-1/2}$<br>D = 203.730 mg $g^{-1}$ | 0.9982 |
| Simple Elovich | $K_E$ = 2.278 mg $g^{-1}$ $min^{-1}$<br>$\beta$ = 0.175 g $mg^{-1}$ | 0.9804 |

## 4. Conclusions

Magnetic carbon nanotubes composite (MWCNTs-$Fe_3O_4$) was synthesized and efficiently used for the adsorption of Hg(II) ions from aqueous solutions. The adsorption capacity depends on the adsorbent dosage, contact time, pH and initial metal ion concentration. The calculated adsorption parameters and the equilibrium data were best fitted by Langmuir model giving a maximum adsorption capacity of 238.78 mg $g^{-1}$. The adsorption process was studied kinetically and the results were analyzed by pseudo-first-order, pseudo-second-order, intraparticle diffusion and simple Elovich models. Pseudo-second-order was found to be the best correlation model

based on the values of the correlation coefficient ($R^2$). This result suggests that MWCNTs-$Fe_3O_4$ prepared in this study could be a promising adsorbent for the removal of Hg(II) ions in waste/water treatment and environmental management applications, in terms of high efficiency and feasibility.

**Acknowledgements**

The authors would like to acknowledge the funding from the Ministry of Higher Education Malaysia in the form of FRGS grant RDU160118 and Universiti Malaysia Pahang grant RDU170357.

**References**

[1] C. Williams, D. Aderhold, R. Edyvean, Comparison between biosorbents for the removal of metal ions from aqueous solutions, Water Res., 32 (1998) 216-224.
[2] K. Kadirvelu, K. Thamaraiselvi, C. Namasivayam, Removal of heavy metals from industrial wastewaters by adsorption onto activated carbon prepared from an agricultural solid waste, Bioresour. Technol., 76 (2001) 63-65.
[3] S. Wang, L. Zhang, L. Wang, Q. Wu, F. Wang, J. Hao, A review of atmospheric mercury emissions, pollution and control in China, Front. Environ. Sci. Eng., 8 (2014) 631-649.
[4] O.A. Habeeb, R. Kanthasamy, G.A.M. Ali, S. Sethupathi, R.B.M. Yunus, Hydrogen sulfide emission sources, regulations, and removal techniques: a review, Rev. Chem. Eng., DOI 10.1515/revce-2017-0004(2017).
[5] V. K. Gupta, Suhas, Application of low-cost adsorbents for dye removal–A review, J. Environ. Manage., 90 (2009) 2313-2342.
[6] J.G. Dean, F.L. Bosqui, K.H. Lanouette, Removing heavy metals from waste water, Environ. Sci. Technol., 6 (1972) 518-522.
[7] V.K. Gupta, I. Ali, T.A. Saleh, A. Nayak, S. Agarwal, Chemical treatment technologies for waste-water recycling—an overview, RSC Adv., 2 (2012) 6380-6388.
[8] N. Tka, M. Jabli, T.A. Saleh, G.A. Salman, Amines modified fibers obtained from natural Populus tremula and their rapid biosorption of Acid Blue 25, J. Mol. Liq., 250 (2018) 423-432.

[9] A. Demirbas, Heavy metal adsorption onto agro-based waste materials: a review, J. Hazard. Mater., 157 (2008) 220-229.
[10] H.H. Abdel Ghafar, G.A.M. Ali, O.A. Fouad, S.A. Makhlouf, Enhancement of adsorption efficiency of methylene blue on $Co_3O_4/SiO_2$ nanocomposite, Desalin. Water Treat., 53 (2013) 2980-2989.
[11] S. Agarwal, H. Sadegh, M. Monajjemi, A.S. Hamdy, G.A.M. Ali, A.O. Memar, R. Shahryari-ghoshekandi, I. Tyagi, V.K. Gupta, Efficient removal of toxic bromothymol blue and methylene blue from wastewater by polyvinyl alcohol, J. Mol. Liq., 218 (2016) 191-197.
[12] A. Stafiej, K. Pyrzynska, Adsorption of heavy metal ions with carbon nanotubes, Sep. Purif. Technol., 58 (2007) 49-52.
[13] K. Zare, V.K. Gupta, O. Moradi, A.S.H. Makhlouf, M. Sillanpää, M.N. Nadagouda, H. Sadegh, R. Shahryari-ghoshekandi, A. Pal, Z.-J. Wang, A comparative study on the basis of adsorption capacity between CNTs and activated carbon as adsorbents for removal of noxious synthetic dyes: a review, J. Nanostruct. Chem., 5 (2015) 227-236.
[14] S. Babel, T.A. Kurniawan, Low-cost adsorbents for heavy metals uptake from contaminated water: a review, J. Hazard. Mater., 97 (2003) 219-243.
[15] O.A. Habeeb, K. Ramesh, G.A.M. Ali, R.M. Yunus, Experimental design technique on removal of hydrogen sulfide using CaO-eggshells dispersed onto palm kernel shell activated carbon: Experiment, optimization, equilibrium and kinetic studies, Journal of Wuhan University of Technology-Mater. Sci. Ed., 32 (2017) 305-320.
[16] W.W. Ngah, M. Hanafiah, Removal of heavy metal ions from wastewater by chemically modified plant wastes as adsorbents: a review, Bioresour. Technol., 99 (2008) 3935-3948.
[17] F. Fu, Q. Wang, Removal of heavy metal ions from wastewaters: a review, J. Environ. Manage., 92 (2011) 407-418.
[18] M.L. Rahman, S.M. Sarkar, M.M. Yusoff, Efficient removal of heavy metals from electroplating wastewater using polymer ligands, Front. Environ. Sci. Eng., 10 (2016) 352-361.
[19] T.A. Saleh, A.A. Al-Absi, Kinetics, isotherms and thermodynamic evaluation of amine functionalized magnetic carbon for methyl red removal from aqueous solutions, J. Mol. Liq., 248 (2017) 577-585.
[20] V.K. Gupta, I. Tyagi, S. Agarwal, H. Sadegh, R. Shahryari-ghoshekandi, M. Yari, O. Yousefi-nejat, Experimental study of surfaces of hydrogel polymers HEMA, HEMA–EEMA–MA, and PVA as adsorbent for removal of azo dyes from liquid phase, J. Mol. Liq., 206 (2015) 129-136.
[21] H. Sadegh, R. Shahryari-ghoshekandi, I. Tyagi, S. Agarwal, V.K. Gupta, Kinetic and thermodynamic studies for alizarin removal from liquid phase using poly-2-hydroxyethyl methacrylate (PHEMA), J. Mol. Liq., 207 (2015) 21-27.
[22] O.A. Habeeb, R. Kanthasamy, G.A.M. Ali, R.B.M. Yunus, Low-cost and eco-friendly activated carbon from modified palm kernel shell for hydrogen sulfide removal from wastewater: adsorption and kinetic studies, Desalin. Water Treat., 84 (2017) 205-214.
[23] M. Hua, S. Zhang, B. Pan, W. Zhang, L. Lv, Q. Zhang, Heavy metal removal from water/wastewater by nanosized metal oxides: a review, J. Hazard. Mater., 211 (2012) 317-331.

[24] S.-H. Huang, D.-H. Chen, Rapid removal of heavy metal cations and anions from aqueous solutions by an amino-functionalized magnetic nano-adsorbent, J. Hazard. Mater., 163 (2009) 174-179.
[25] H. Sadegh, G.A.M. Ali, V.K. Gupta, A.S.H. Makhlouf, R. Shahryari-ghoshekandi, M.N. Nadagouda, M. Sillanpää, E. Megiel, The role of nanomaterials as effective adsorbents and their applications in wastewater treatment, J. Nanostruct. Chem., 7 (2017) 1-14.
[26] O. Moradi, H. Sadegh, R. Shahryari-Ghoshekandi, M. Norouzi, Application of carbon nanotubes in nanomedicine: new medical approach for tomorrow, 2015.
[27] H. Sadegh, G.A.M. Ali, Z. Abbasi, M.N. Nadagoud, Adsorption of ammonium ions onto multi-walled carbon nanotubes, Studia Universitatis Babes-Bolyai Chemia, 62 (2017) 233-245.
[28] A. Mehrizad, M. Aghaie, P. Gharbani, S. Dastmalchi, M. Monajjemi, K. Zare, Comparison of 4-chloro-2-nitrophenol adsorption on single-walled and multi-walled carbon nanotubes, J. Environ. Health Sci. Eng., 9 (2012) 1-6.
[29] J.L. Bahr, E.T. Mickelson, M.J. Bronikowski, R.E. Smalley, J.M. Tour, Dissolution of small diameter single-wall carbon nanotubes in organic solvents?, Chem. Commun., 2 (2001) 193-194.
[30] F. Mollaamin, M. Monajjemi, Fractal dimension on carbon nanotube-polymer composite materials using percolation theory, J. Comput. Theor. Nanosci., 9 (2012) 597-601.
[31] S. Singh, K. Barick, D. Bahadur, Functional oxide nanomaterials and nanocomposites for the removal of heavy metals and dyes, Nanomater. Nanotechnol., 3 (2013) 1-19.
[32] H. Gu, H. Lou, J. Tian, S. Liu, Y. Tang, Reproducible magnetic carbon nanocomposites derived from polystyrene with superior tetrabromobisphenol A adsorption performance, J. Mater. Chem., A, 4 (2016) 10174-10185.
[33] J. Zhu, H. Gu, J. Guo, M. Chen, H. Wei, Z. Luo, H.A. Colorado, N. Yerra, D. Ding, T.C. Ho, N. Haldolaarachchige, J. Hopper, D.P. Young, Z. Guo, S. Wei, Mesoporous magnetic carbon nanocomposite fabrics for highly efficient Cr(VI) removal, J. Mater. Chem., A, 2 (2014) 2256-2265.
[34] H. Gu, H. Lou, D. Ling, B. Xiang, Z. Guo, Polystyrene controlled growth of zerovalent nanoiron/magnetite on a sponge-like carbon matrix towards effective Cr(VI) removal from polluted water, RSC Adv., 6 (2016) 110134-110145.
[35] H. Sadegh, R. Shahryari-ghoshekandi, M. Kazemi, Study in synthesis and characterization of carbon nanotubes decorated by magnetic iron oxide nanoparticles, Int. Nano Lett., 4 (2014) 129-135.
[36] K. Zare, H. Sadegh, R. Shahryari-ghoshekandi, M. Asif, I. Tyagi, S. Agarwal, V.K. Gupta, Equilibrium and kinetic study of ammonium ion adsorption by $Fe_3O_4$ nanoparticles from aqueous solutions, J. Mol. Liq., 213 (2016) 345-350.
[37] S. Kanagesan, M. Hashim, S. Tamilselvan, N. Alitheen, I. Ismail, A. Hajalilou, K. Ahsanul, Synthesis, characterization, and cytotoxicity of iron oxide nanoparticles, Adv. Mater. Sci. Eng., 2013 (2013) 1-7.
[38] X.-J. Fan, L. Xin, Preparation and magnetic property of multiwalled carbon nanotubes decorated by $Fe_3O_4$ nanoparticles, New Carbon Mater., 27 (2012) 111-116.

[39] F. He, J. Fan, D. Ma, L. Zhang, C. Leung, H.L. Chan, The attachment of $Fe_3O_4$ nanoparticles to graphene oxide by covalent bonding, Carbon, 48 (2010) 3139-3144.

[40] A. Patterson, The Scherrer formula for X□ray particle size determination, Phys. Rev., 56 (1939) 978□982.

[41] P.R. Chang, P. Zheng, B. Liu, D.P. Anderson, J. Yu, X. Ma, Characterization of magnetic soluble starch-functionalized carbon nanotubes and its application for the adsorption of the dyes, J. Hazard. Mater., 186 (2011) 2144-2150.

[42] Z. Yao, N. Braidy, G.A. Botton, A. Adronov, Polymerization from the surface of single-walled carbon nanotubes-preparation and characterization of nanocomposites, J. Am. Chem. Soc., 125 (2003) 16015-16024.

[43] S. Song, R. Rao, H. Yang, H. Liu, A. Zhang, Facile synthesis of Fe3O4/MWCNTs by spontaneous redox and their catalytic performance, Nanotechnology, 21 (2010) 185602.

[44] O. Moradi, K. Zare, Adsorption of Pb (II), Cd (II) and Cu (II) ions in aqueous solution on SWCNTs and SWCNT–COOH surfaces: kinetics studies, Fullerenes Nanotubes Carbon Nanostruct., 19 (2011) 628-652.

[45] O. Moradi, K. Zare, M. Yari, Interaction of some heavy metal ions with single walled carbon nanotube, Int. J. Nano Dimens., 1 (2011) 203-220.

[46] A.K. Singha Deb, V. Dwivedi, K. Dasgupta, S. Musharaf Ali, K.T. Shenoy, Novel amidoamine functionalized multi-walled carbon nanotubes for removal of mercury(II) ions from wastewater: Combined experimental and density functional theoretical approach, Chem. Eng. J., 313 (2017) 899-911.

[47] D.H.K. Reddy, S.-M. Lee, Application of magnetic chitosan composites for the removal of toxic metal and dyes from aqueous solutions, Adv. Colloid Interface Sci., 201 (2013) 68-93.

[48] V.K. Gupta, O. Moradi, I. Tyagi, S. Agarwal, H. Sadegh, R. Shahryari-Ghoshekandi, A. Makhlouf, M. Goodarzi, A. Garshasbi, Study on the removal of heavy metal ions from industry waste by carbon nanotubes: effect of the surface modification: a review, Crit. Rev. Env. Sci. Technol., DOI 10.1080/10643389.2015.1061874(2015) DOI: 10.1080/10643389.10642015.11061874.

[49] H. Sadegh, R. Shahryari-ghoshekandi, S. Agarwal, I. Tyagi, M. Asif, V.K. Gupta, Microwave-assisted removal of malachite green by carboxylate functionalized multi-walled carbon nanotubes: Kinetics and equilibrium study, J. Mol. Liq., 206 (2015) 151-158.

[50] V.K. Thakur, M.K. Thakur, Chemical Functionalization of Carbon Nanomaterials: Chemistry and Applications, CRC Press2015.

[51] T.A. Saleh, Nanocomposite of carbon nanotubes/silica nanoparticles and their use for adsorption of Pb(II): from surface properties to sorption mechanism, Desalin. Water Treat., 57 (2016) 10730-10744.

[52] T.A. Seaf Elnsar, M.H. Soliman, M.A.-E.-A.A. Ayash, Modified hydroxyapatite adsorbent for removal of iron dissolved in water wells in Sohag, Egypt, Chem. Adv. Mater., 2 (2017) 1-13.

[53] A.S. Özcan, B. Erdem, A. Özcan, Adsorption of Acid Blue 193 from aqueous solutions onto BTMA-bentonite, Colloids Surf., A, 266 (2005) 73-81.
[54] R. Sivaraj, C. Namasivayam, K. Kadirvelu, Orange peel as an adsorbent in the removal of acid violet 17 (acid dye) from aqueous solutions, Waste Manage. (Oxford), 21 (2001) 105-110.
[55] O.A. Habeeb, K. Ramesh, G.A.M. Ali, R.M. Yunus, Isothermal modelling based experimental study of dissolved hydrogen sulfide adsorption from waste water using eggshell based activated carbon, Malaysian J. Anal. Sci., 21 (2017) 334-345.
[56] K. Jainae, N. Sukpirom, S. Fuangswasdi, F. Unob, Adsorption of Hg(II) from aqueous solutions by thiol-functionalized polymer-coated magnetic particles, J. Ind. Eng. Chem., 23 (2015) 273-278.
[57] Z. Wang, J. Xu, Y. Hu, H. Zhao, J. Zhou, Y. Liu, Z. Lou, X. Xu, Functional nanomaterials: Study on aqueous Hg(II) adsorption by magnetic $Fe_3O_4$@$SiO_2$-SH nanoparticles, Journal of the Taiwan Institute of Chemical Engineers, 60 (2016) 394-402.
[58] J. Song, H. Kong, J. Jang, Adsorption of heavy metal ions from aqueous solution by polyrhodanine-encapsulated magnetic nanoparticles, J. Colloid Interface Sci., 359 (2011) 505-511.
[59] M. Sun, G. Cheng, X. Ge, M. Chen, C. Wang, L. Lou, X. Xu, Aqueous Hg(II) immobilization by chitosan stabilized magnetic iron sulfide nanoparticles, Sci. Total Environ., DOI https://doi.org/10.1016/j.scitotenv.2017.10.119(2017).
[60] M. Anbia, S. Amirmahmoodi, Removal of Hg (II) and Mn (II) from aqueous solution using nanoporous carbon impregnated with surfactants, Arabian J. Chem., 9 (2016) S319-S325.
[61] N.M. Bandaru, N. Reta, H. Dalal, A.V. Ellis, J. Shapter, N.H. Voelcker, Enhanced adsorption of mercury ions on thiol derivatized single wall carbon nanotubes, J. Hazard. Mater., 261 (2013) 534-541.
[62] A.H. El-Sheikh, Y.S. Al-Degs, R.M. Al-As'ad, J.A. Sweileh, Effect of oxidation and geometrical dimensions of carbon nanotubes on Hg(II) sorption and preconcentration from real waters, Desalination, 270 (2011) 214-220.
[63] H. Alijani, Z. Shariatinia, A. Aroujalian Mashhadi, Water assisted synthesis of MWCNTs over natural magnetic rock: An effective magnetic adsorbent with enhanced mercury(II) adsorption property, Chem. Eng. J., 281 (2015) 468-481.
[64] M. Hadavifar, N. Bahramifar, H. Younesi, Q. Li, Adsorption of mercury ions from synthetic and real wastewater aqueous solution by functionalized multi-walled carbon nanotube with both amino and thiolated groups, Chem. Eng. J., 237 (2014) 217-228.
[65] Y.-S. Ho, Review of second-order models for adsorption systems, J. Hazard. Mater., 136 (2006) 681-689.
[66] T. A. Saleh, A. Sarı, M. Tuzen, Chitosan-modified vermiculite for As(III) adsorption from aqueous solution: Equilibrium, thermodynamic and kinetic studies, J. Mol. Liq., 219 (2016) 937-945.
[67] Y.-S. Ho, G. McKay, Pseudo-second order model for sorption processes, Process Biochem., 34 (1999) 451-465.
[68] T.A. Saleh, Mercury sorption by silica/carbon nanotubes and silica/activated carbon: a comparison study, Journal of Water Supply: Research and Technology - Aqua, 64 (2015) 892-903.

[69] K. Zare, H. Sadegh, R. Shahryari-ghoshekandi, B. Maazinejad, V. Ali, I. Tyagi, S. Agarwal, V.K. Gupta, Enhanced removal of toxic Congo red dye using multi walled carbon nanotubes: Kinetic, equilibrium studies and its comparison with other adsorbents, J. Mol. Liq., 212 (2015) 266-271.

[70] V.K. Gupta, S. Agarwal, H. Sadegh, G.A.M. Ali, A.K. Bharti, A.S. Hamdy, Facile route synthesis of novel graphene oxide-β-cyclodextrin nanocomposite and its application as adsorbent for removal of toxic bisphenol A from the aqueous phase, J. Mol. Liq., 237 (2017) 466–472.

[71] V. Gupta, I. Tyagi, H. Sadegh, R. Shahryari-Ghoshekandi, A. Makhlouf, B. Maazinejad, Nanoparticles as adsorbent; a positive approach for removal of noxious metal ions: a review, Sci. Technol. Dev., 34 (2015) 195-214.

## Highlights

- MWCNTs-$Fe_3O_4$ nanocomposite was successfully prepared and characterized.
- MWCNTs-$Fe_3O_4$ showed suburb adsorption performance toward Hg(II).
- MWCNTs-$Fe_3O_4$ showed high Hg(II) adsorption capacity of 238.78 mg $g^{-1}$.
- The results recommend the successful application of MWCNTs-$Fe_3O_4$ for Hg(II) removal.

## Graphical Abstract